Annals of the University of Craiova, Mathematics and Computer Science Series
Volume 51(1), 2024, Pages 54–81, DOI: 10.52846/ami.v51i1.1744
ISSN: 1223-6934

An Inverse Problem of Reconstructing the Unknown Coefficient in a Third Order Time Fractional Pseudoparabolic Equation

Mousa J. Huntul, Ibrahim Tekin, Muhammad K. Iqbal, and Muhammad Abbas

Abstract. In this paper, we have considered the problem of reconstructing the time dependent potential term for the third order time fractional pseudoparabolic equation from an additional data at the left boundary of the space interval. This is very challenging and interesting inverse problem with many important applications in various fields of engineering, mechanics and physics. The existence of unique solution to the problem has been discussed by means of the contraction principle on a small time interval and the unique solvability theorem is proved. The stability results for the inverse problem have also been presented. However, since the governing equation is yet ill-posed (very slight errors in the additional input may cause relatively significant errors in the output potential), the regularization of the solution is needed. Therefore, to get a stable solution, a regularized objective function is to be minimized for retrieval of the unknown coefficient of the potential term. The proposed problem is discretized using the cubic B-spline (CB-spline) collocation technique and has been reshaped as a non-linear least-squares optimization of the Tikhonov regularization function. The stability analysis of the direct numerical scheme has also been presented. The MATLAB subroutine *lsqnonlin* tool has been used to expedite the numerical computations. Both perturbed data and analytical are inverted and the numerical outcomes for two benchmark test examples are reported and discussed.

2010 Mathematics Subject Classification. Primary 35R30; Secondary 65K10, 35A02.
Key words and phrases. Inverse problem, Fractional derivative, Pseudo-parabolic equation, Tikhonov regularization, Stability analysis, Nonlinear optimization.

1. Introduction

Fractional partial differential equations are cropped up in mathematical modelling of a wide range of natural phenomena and dynamic processes in science and engineering such as plate deviation theory, fluids flows in lungs, episodic vibration of a elastic beams, physical flows including ice formation, noise removal and edge preservation in images, oscillation control in bridge slabs, floor systems, large window glasses and airplane wings [2, 7, 12, 24, 25]. Time-fractional in a higher-order pseudo-parabolic equations have been used as a major tool for modelling various practical fields and there are a number of publications devoted to the study of time-fractional PDEs and their applications, see [5,17,21] to mention only a few. The fractional order linearized Mullins sub-diffusion model was first studied by Hamed and Nepomnyashchy [8] by simply replacing the integer order derivative with the non-integer one.

Received March 8, 2023. Accepted October 9, 2023.

The inverse problems of identifying time dependent surface diffusion term of the higher-order pseudoparabolic equation from total mass measurement of the profile at an arbitrary fixed point in space interval is studied in [14]. The authors in [19, 20] considered the problem of finding the time dependent lowest term for the third order pseudoparabolic equation subject to various boundary conditions. Huntul et al. [10, 11] considered a fourth order pseudoparabolic inverse problem with some additional information and identified the unknown time dependent potential coefficient. Aziz and Salman [6] considered two inverse problems on fourth order parabolic equation involving Hilfer fractional derivative. The authors retrieved the space dependant forcing term from the known data and recovered the time dependant source from the over determined condition of integral type. The existence of unique solutions and stability results for both inverse problems were also derived. Huntul et al. [9] studied the reconstruction of unknown time and space dependent coefficients in third-order pseudoparabolic inverse problems subject to nonlocal integral conditions. Recently, the direct and inverse problems for the time fractional pseudoparabolic equation with different abstract self-adjoint operators have been studied by Ruzhansky *et al.* [23]. However, the work on inverse problems for third order time fractional pseudo-parabolic equations is scarce.

In this article, we study the third order time fractional pseudoparabolic problem to reconstruct the time dependent potential term along with the solution function theoretically, i.e. existence and uniqueness, and numerically, for the first time, in the prescribed domain using the initial and Dirichlet boundary conditions, and the additional data at the left boundary of the space interval as an over-determination condition. The stability results for the inverse problem is proved. The preeminent goal of the current work is to undertake the theory and numerical aspect of this problem.

The article is organized as follows. The proposed inverse problem has been mathematically developed in Section 2. In Section 3, we present some preliminary lemmas that have been in the following sections. The existence and uniqueness of a solution of the inverse problem on a sufficiently small time interval by using the contraction principle are proved in Section 4. Section 5 briefly explains the scheme for solving the direct problem by means of CB-spline collocation technique. The unconditional stability has been proved in Section 6. The description of numerical procedure to solve the minimization of the nonlinear Tikhonov regularization functional has been given in Section 7. The computational outcomes for some examples on the topic are discussed in Section 8. Finally, concluding remarks are revealed in Section 9.

2. Mathematical formulation of the inverse problem

We consider an inverse problem of reconstructing the time dependent potential coefficient $a(\tau)$ in a third-order time-fractional pseudo-parabolic equation

$$\frac{\partial^\alpha z(\kappa,\tau)}{\partial \tau^\alpha} - \frac{\partial^3 z(\kappa,\tau)}{\partial \kappa^2 \partial \tau} = f(\kappa,\tau) + a(\tau) z(\kappa,\tau), \quad (\kappa,\tau) \in (0,\ell) \times [0,T], \tag{1}$$

subject to

$$z(\kappa,0) = \xi(\kappa), \quad \kappa \in [0,\ell], \tag{2}$$

the Dirichlet type of boundary conditions

$$z(0,\tau) = z(\ell,\tau) = 0, \quad \tau \in [0,T], \tag{3}$$

and the additional data

$$z(X_0,\tau) = r(\tau), \quad X_0 \in (0,\ell), \quad \tau \in [0,T], \tag{4}$$

where $\frac{\partial^\alpha}{\partial \tau^\alpha}$ is the Caputo fractional derivative (CFD) operator with singular kernel and is defined as [22]

$$\frac{\partial^\alpha z(\kappa,\tau)}{\partial \tau^\alpha} = \frac{1}{\Gamma(1-\alpha)} \int_0^\tau \frac{1}{(\tau-s)^\alpha} \frac{\partial z(\kappa,s)}{\partial s} ds, \quad \alpha \in (0,1),$$

where $\Gamma(\cdot)$ represents Gamma function.

3. Preliminaries

Throughout this article, the following definition and lemmas are used:

Definition 3.1 ([16]). The generalized Mittag-Leffler function is defined by

$$E_{\alpha,\beta}(z) = \sum_{k=0}^{\infty} \frac{z^k}{\Gamma(\alpha k+\beta)}, \ z \in \mathbb{C},$$

where $\alpha > 0$, $\beta \in \mathbb{R}$.

Lemma 3.1 ([16, 22]). *Let $0 < \alpha < 1$, and $\beta \in \mathbb{R}$ be arbitrary. We suppose that μ is such that $\frac{\pi\alpha}{2} < \mu < \min\{\pi, \pi\alpha\}$. Then, $\exists$ a constant $C_{\alpha,\beta}$ such that*

$$|E_{\alpha,\beta}(z)| \le \frac{C_{\alpha,\beta}}{1+|z|}, \ \mu \le |\arg(z)| \le \pi.$$

Lemma 3.2 ([22]). *Let $\alpha > 0$, $\beta > 0$. Then*

$$\int_0^\infty e^{-zt} t^{\beta-1} E_{\alpha,\beta}(\pm a t^\alpha) dt = \frac{\tau^{\alpha-\beta}}{\tau^\alpha \mp a}, \ Re(\tau) > |a|^{\frac{1}{\alpha}}.$$

Lemma 3.3 ([4, 22]). *Let $\alpha > 0$, $\beta > 0$. Then*

$$\frac{d}{dt} t^{\beta-1} E_{\alpha,\beta}(a t^\alpha) = t^{\beta-2} E_{\alpha,\beta-1}(a t^\alpha).$$

Lemma 3.4 ([4]). *Let $\alpha > 0$. Then*

$$\frac{d}{dt} E_{\alpha,1}(t^\alpha) = t^{\alpha-1} E_{\alpha,\alpha}(t^\alpha).$$

Lemma 3.5 ([22]). *Let $Re(s) > 0$. Then for $0 < \alpha < 1$ we have*

$$\mathcal{L}\left\{\frac{\partial^\alpha f(t)}{\partial t^\alpha}\right\} = s^\alpha \mathcal{F}(s) - s^{\alpha-1} f(0),$$

where $\mathcal{F}(s)$ is the Laplace transform of $f(t)$.

4. Solvability of the problem

We define a Banach space corresponding to the eigenfunctions and eigenvalues of the auxiliary spectral problem of (1)–(4). Then, we set and prove the existence and uniqueness theorem of the solution of the inverse initial-boundary value problem for the time fractional pseudo parabolic equation (1) by using Banach fixed point theorem in this space.

Definition 4.1. A solution of the problem (1)–(4), which called the classical solution, is a pair of functions $\{a(\tau), z(\kappa,\tau)\}$ satisfying $z(\kappa,\tau) \in C^2([0,\ell],\mathbb{R})$, $a(\tau) \in C[0,T]$, and $\frac{\partial^\alpha z(\kappa,\tau)}{\partial\tau^\alpha} \in C([0,T],\mathbb{R})$.

We apply the Fourier method to obtain the solution of the problem (1)–(4) since the boundary conditions are homogeneous. The auxiliary spectral problem is considered by

$$\begin{cases} Y''(\kappa) + \lambda Y(\kappa) = 0, \quad \kappa \in [0,\ell], \\ Y(0) = Y(\ell) = 0. \end{cases} \tag{5}$$

This spectral problem has the eigenfunctions $Y_n(\kappa) = \sqrt{\frac{2}{\ell}}\sin(\sqrt{\lambda_n}\kappa)$, $n = 1, 2, ...$, and eigenvalues $\lambda_n = \left(\frac{n\pi}{\ell}\right)^2$.

In the rest of the article, we will consider following spaces to investigate the solution of the problem (1)–(4).

I::

$$B_T = \Bigg\{ z(\kappa,\tau) = \sum_{n=1}^{\infty} z_n(\tau) Y_n(\kappa) : \ z_n(\tau) \in C[0,T], \\ J_T(z) = \left[\sum_{n=1}^{\infty} \left(\lambda_n^{5/2} \max_{0\le\tau\le T} |z_n(\tau)| \right)^2 \right]^{1/2} < +\infty \Bigg\}$$

with the norm $\|z(\kappa,\tau)\|_{B_T} \equiv J_T(z)$. This space is related to the Fourier coefficients of the function $z(\kappa,\tau)$ is obtained by using the eigenfunctions $Y_n(\kappa)$, $n = 1, 2, ...$ It is easy to shown that B_T is a Banach space.

II:: $E_T = B_T \times C[0,T]$ of the vector function $w = [a(\tau), z(\kappa,\tau)]^T$ with the norm

$$\|w\|_{E_T} = \|a(\tau)\|_{C[0,T]} + \|z(\kappa,\tau)\|_{B_T},$$

where E_T represents Banach space.

Theorem 4.1. *Suppose that the following conditions hold:*
(A$_1$): $\xi(\kappa) \in C^5[0,\ell]$, $\xi''(0) = \xi''(\ell) = \xi(0) = \xi(\ell) = 0$;
(A$_2$): $r(\tau) \in C^1[0,T]$, $r(\tau) \ne 0, \forall\tau \in [0,T]$, $r(0) = \xi(X_0)$, $\frac{\partial^\alpha r(\tau)}{\partial\tau^\alpha} \in C[0,T]$;
(A$_3$): $f(\kappa,\tau) \in C^{3,0}(\overline{D}_T)$, $f_{\kappa\kappa}(0,\tau) = f_{\kappa\kappa}(\ell,\tau) = f(0,\tau) = f(\ell,\tau) = 0$.
Then, the problem (1)–(4) has a unique solution for small time.

Proof. Let us seek the solution of the problem (1)–(4) in terms of the eigenfunction basis

$$z(\kappa,\tau) = \sum_{n=1}^{\infty} z_n(\tau) Y_n(\kappa), \tag{6}$$

where

$$z_n(\tau) = \int_0^\ell z(\kappa,\tau)Y_n(\kappa)d\kappa.$$

Since (6) is the solution of the problem (1)–(4), $z_n(\tau)$ satisfy the following initial value problems:

$$\begin{cases} \frac{\partial^\alpha z_n(\tau)}{\partial \tau^\alpha} + \lambda_n z_n(\tau) = F_n(\tau;a,z), \quad 0 \le \tau \le T, \\ z_n(0) = \xi_n, \ n = 1,2,..., \end{cases} \tag{7}$$

where

$$F_n(\tau;a,z) = f_n(\tau) + a(\tau)z_n(\tau), \ \xi_n = \int_0^1 \xi(\kappa)Y_n(\kappa)d\kappa, \ f_n(\tau) = \int_0^\ell f(\kappa,\tau)Y_n(\kappa)d\kappa.$$

The Laplace transform of both sides of (7) yields

$$Z_n(s) = \frac{s^{\alpha-1}+\lambda_n}{s^\alpha+\lambda_n s}\xi_n + \frac{\mathcal{F}_n(s;a,z)}{s^\alpha+\lambda_n s}. \tag{8}$$

Before taking the inverse Laplace transform, let us rewrite the last equality as

$$Z_n(s) = \left(\frac{s^{\alpha-2}}{s^{\alpha-1}+\lambda_n} + \lambda_n \frac{s^1}{s^{\alpha-1}+\lambda_n}\right)\xi_n + \frac{s^{-1}}{s^{\alpha-1}+\lambda_n}\mathcal{F}_n(s;a,z). \tag{9}$$

By using the inverse Laplace by using Lemma 2, we obtain the solutions of the Cauchy problems (7)

$$\begin{aligned} z_n(\tau) = & \left[\lambda_n \tau^{\alpha-1} E_{\alpha-1,\alpha}(-\lambda_n \tau^{\alpha-1}) + E_{\alpha-1,1}(-\lambda_n \tau^{\alpha-1})\right]\xi_n \\ & + \int_0^\tau (\tau-s)^{\alpha-1} E_{\alpha-1,\alpha}(-\lambda_n (\tau-s)^\alpha) F_n(s;a,z)ds. \end{aligned} \tag{10}$$

Considering (10) into (6), we obtain

$$\begin{aligned} z(\kappa,\tau) = & \sum_{n=1}^\infty \left[\left[\lambda_n \tau^{\alpha-1} E_{\alpha-1,\alpha}(-\lambda_n \tau^{\alpha-1}) + E_{\alpha-1,1}(-\lambda_n \tau^{\alpha-1})\right]\xi_n\right. \\ & + \int_0^\tau (\tau-s)^{\alpha-1} E_{\alpha-1,\alpha}(-\lambda_n (\tau-s)^\alpha) F_n(s;a,z)dsY_n(\kappa). \end{aligned} \tag{11}$$

For reconstruction of $a(\tau)$, we derive

$$a(\tau) = \frac{1}{r(\tau)}\left[\frac{\partial^\alpha r(\tau)}{\partial \tau^\alpha} - \frac{\partial^3 z(X_0,\tau)}{\partial \kappa^2 \partial \tau} - f(X_0,\tau)\right] \tag{12}$$

from the equation (1) with the additional data (4). Considering the equation (11) in the last equation of $a(\tau)$, we obtain

$$a(\tau) = \frac{1}{r(\tau)}\left[\frac{\partial^\alpha r(\tau)}{\partial \tau^\alpha} - f(X_0,\tau) + \sum_{n=1}^\infty \lambda_n z_n'(\tau)Y_n(X_0)\right], \tag{13}$$

or, we can rewrite more wider as

$$\begin{aligned} a(\tau) = \frac{1}{r(\tau)} & \left[\frac{\partial^\alpha r(\tau)}{\partial \tau^\alpha} - f(X_0,\tau) + \sum_{n=1}^\infty \lambda_n \left([1+\lambda_n]\tau^{\alpha-2} E_{\alpha-1,\alpha-1}(-\lambda_n \tau^{\alpha-1})\xi_n\right.\right. \\ & \left.\left. + \int_0^\tau (\tau-s)^{\alpha-2} E_{\alpha-1,\alpha-1}(-\lambda_n (\tau-s)^\alpha) F_n(s;a,z)ds\right) Y_n(X_0)\right]. \end{aligned} \tag{14}$$

Thus, we reduced solving the problem (1)–(4) to solving the system (11)–(13) with respect to unknown functions $a(\tau)$ and $z(\kappa,\tau)$.

Now, let us denote $w = [z(\kappa,\tau), a(\tau)]^T$ and rewrite the system of equations (11)–(13) in the operator form

$$w = \Theta(w), \tag{15}$$

where $\Theta = [\theta_1, \theta_2]^T$ and θ_1 and θ_2 are equal to the right hand sides of (11) and (13), respectively, as

$$\theta_1(w) = \sum_{n=1}^{\infty} z_n(\tau) Y_n(\kappa), \tag{16}$$

$$\theta_2(w) = \frac{1}{r(\tau)} \left[\frac{\partial^\alpha r(\tau)}{\partial \tau^\alpha} - f(X_0,\tau) + \sum_{n=1}^{\infty} \lambda_n z_n'(\tau) Y_n(X_0) \right], \tag{17}$$

where

$$z_n(\tau) = \int_0^\tau (\tau - s)^{\alpha-1} E_{\alpha-1,\alpha}(-\lambda_n (\tau-s)^\alpha) F_n(s;a,z) ds + \left[E_{\alpha-1,1}(-\lambda_n \tau^{\alpha-1}) + \lambda_n \tau^{\alpha-1} E_{\alpha-1,\alpha}(-\lambda_n \tau^{\alpha-1}) \right] \xi_n,$$

and

$$z_n'(\tau) = \int_0^\tau (\tau - s)^{\alpha-2} E_{\alpha-1,\alpha-1}(-\lambda_n (\tau-s)^\alpha) F_n(s;a,z) ds + [1+\lambda_n] \tau^{\alpha-2} E_{\alpha-1,\alpha-1}(-\lambda_n \tau^{\alpha-1}) \xi_n.$$

To apply Banach fixed point theorem first we need to demonstrate that Θ maps E_T onto itself continuously. In other words, let us show that $\theta_1(w) \in B_T$ and $\theta_2(w) \in C[0,T]$ for arbitrary $w = [z(\kappa,\tau), a(\tau)]^T$ by considering $a(\tau) \in C[0,T]$, $z(\kappa,\tau) \in B_T$.

Before proving Θ maps E_T onto itself continuously, let us give some equalities which are important to apply Bessel inequality. By using integration by parts under the assumptions (A_1)-(A_3), it easy to see that

$$f_n(\tau) = \frac{1}{\lambda_n^{3/2}} B_n(\tau), \quad \xi_n = \frac{1}{\lambda_n^{5/2}} A_n, \tag{18}$$

where

$$A_n = \sqrt{\frac{2}{\ell}} \int_0^\ell \xi^{(5)}(x) \cos\left(\sqrt{\lambda_n}\kappa\right) d\kappa, \; B_n(\tau) = -\sqrt{\frac{2}{\ell}} \int_0^\ell f_{\kappa\kappa\kappa}(\kappa,\tau) \sin\left(\sqrt{\lambda_n}\kappa\right) d\kappa.$$

Also, let us consider $\widehat{C} = \max\{C_{\alpha-1,1}, C_{\alpha-1,\alpha}, C_{\alpha-1,\alpha-1}\}$, where $C_{\alpha-1,1}$, $C_{\alpha-1,\alpha}$, $C_{\alpha-1,\alpha-1}$ are the upper bound coefficients of the Mittag-Leffler functions $E_{\alpha-1,1}$, $E_{\alpha-1,\alpha}$, $E_{\alpha-1,\alpha-1}$, respectively.

First, let us show that $\theta_1(w) \in B_T$, in other words we need to show

$$J_T(\theta_1) = \left[\sum_{n=1}^{\infty} \left(\lambda_n^{5/2} \max_{0\le\tau\le T} |\theta_{1n}(\tau)| \right)^2 \right]^{1/2} < +\infty, \tag{19}$$

where

$$\theta_{1n}(\tau) = \int_0^\tau (\tau - s)^{\alpha-1} E_{\alpha-1,\alpha}(-\lambda_n (\tau-s)^\alpha) F_n(s;a,z) ds + \left[E_{\alpha-1,1}(-\lambda_n \tau^{\alpha-1}) + \lambda_n \tau^{\alpha-1} E_{\alpha-1,\alpha}(-\lambda_n \tau^{\alpha-1}) \right] \xi_n.$$

Taking the absolute value both sides and applying Lemma 3.1, we have

$$\begin{aligned}
|\theta_{1n}(\tau)| \leq & \left[\left|E_{\alpha-1,1}(-\lambda_n\tau^{\alpha-1})\right| + \left|\lambda_n\tau^{\alpha-1}E_{\alpha-1,\alpha}(-\lambda_n\tau^{\alpha-1})\right|\right]|\xi_n| \\
& + \int_0^\tau \left|(\tau-s)^{\alpha-1}E_{\alpha-1,\alpha}(-\lambda_n(\tau-s)^\alpha)\right| |F_n(s;a,z)|\,ds \\
\leq & \left[\frac{C_{\alpha-1,1}}{1+\lambda_n\tau^{\alpha-1}} + \lambda_n\tau^{\alpha-1}\frac{C_{\alpha-1,\alpha}}{1+\lambda_n\tau^{\alpha-1}}\right]|\xi_n| \\
& + \int_0^\tau |\tau-s|^{\alpha-1}\frac{C_{\alpha-1,\alpha}}{1+\lambda_n|\tau-s|^{\alpha-1}}|F_n(s;a,z)|\,ds \\
\leq & \widehat{C}|\xi_n| + \int_0^T |\tau-s|^{\alpha-1}\frac{\widehat{C}}{\lambda_n|\tau-s|^{\alpha-1}}|F_n(s;a,z)|\,ds \\
\leq & \widehat{C}\left\{|\xi_n| + \frac{T}{\lambda_n}\left[|a(\tau)||z_n(\tau)| + |f_n(\tau)|\right]\right\}.
\end{aligned}$$

Under the assumptions (A_1)-(A_3), we get from the last inequality

$$\begin{aligned}
\sum_{n=1}^{\infty}\left(\lambda_n^{5/2}\max_{0\leq\tau\leq T}|\theta_{1n}(\tau)|\right)^2 \leq & 2\widehat{C}^2\left\{\sum_{n=1}^{\infty}|A_n|^2 + T^2\sum_{n=1}^{\infty}\left(\max_{0\leq\tau\leq T}|B_n(\tau)|\right)^2\right. \\
& \left. +T^2\left(\max_{0\leq\tau\leq T}|a(\tau)|\right)^2\sum_{n=1}^{\infty}\left(\lambda_n^{5/2}\max_{0\leq\tau\leq T}|z_n(\tau)|\right)^2\right\}. \qquad (20)
\end{aligned}$$

From the Bessel inequality and $a(\tau) \in C[0,T]$, $z(\kappa,\tau) \in B_T$, the series on the right side of the (20) are convergent. Thus $J_T(\theta_1) < +\infty$ and $\theta_1(w)$ is belongs to the space B_T.

Now, let us show that $\theta_2(w) \in C[0,T]$. Taking the absolute value both sides of the equation (17), we obtain

$$\begin{aligned}
|\theta_2(w)| \leq & \frac{1}{|r(\tau)|}\left[\left|\frac{\partial^\alpha r(\tau)}{\partial\tau^\alpha}\right| + |f(X_0,\tau)|\right. \\
& + \sum_{n=1}^{\infty}\lambda_n\left([1+\lambda_n]\left|\tau^{\alpha-2}E_{\alpha-1,\alpha-1}(-\lambda_n\tau^{\alpha-1})\xi_n\right|\right. \\
& \left.\left. + \int_0^\tau |\tau-s|^{\alpha-2}|E_{\alpha-1,\alpha-1}(-\lambda_n(\tau-s)^\alpha)||F_n(s;a,z)|\,ds\right)\right].
\end{aligned}$$

Since $\lambda_n > 0$, $n = 1, 2, ...$, $\lambda_n(1+\lambda_n) \leq 2\lambda_n^2$. Then, we obtain

$$\begin{aligned}
|\theta_2(w)| \leq & \frac{1}{\min_{0\leq\tau\leq T}|r(\tau)|}\left[\left|\frac{\partial^\alpha r(\tau)}{\partial\tau^\alpha}\right| + |f(X_0,\tau)|\right. \\
& + \sum_{n=1}^{\infty}\left(2\lambda_n^2T^{\alpha-2}\frac{\widehat{C}}{1+\lambda_n\tau^{\alpha-1}}|\xi_n|\right. \\
& \left.\left. +\lambda_n\int_0^T |\tau-s|^{\alpha-2}\frac{\widehat{C}}{1+\lambda_n|\tau-s|^{\alpha-1}}|F_n(s;a,z)|\,ds\right)\right]
\end{aligned}$$

by considering Lemma 3.1. Under the assumptions (A_1)-(A_3), using Cauchy-Schwartz and Bessel inequalities, analogously, we have

$$\begin{aligned}\underset{0\le\tau\le T}{max}|\theta_2(w)| \le \frac{1}{\underset{0\le\tau\le T}{min}|r(\tau)|}\Bigg[\underset{0\le\tau\le T}{max}\left|\frac{\partial^\alpha h(\tau)}{\partial\tau^\alpha}\right| + \underset{0\le\tau\le T}{max}|f(X_0,\tau)| \\ + \left(\sum_{n=1}^{\infty}\frac{1}{\lambda_n}\right)^{1/2}\widehat{C}\left\{2T^{\alpha-2}\left(\sum_{n=1}^{\infty}|A_n|^2\right)^{1/2} + T\left(\sum_{n=1}^{\infty}\left(\underset{0\le\tau\le T}{max}|B_n(\tau)|\right)^2\right)^{1/2}\right\} \\ +\widehat{C}\left(\sum_{n=1}^{\infty}\frac{1}{\lambda_n^3}\right)^{1/2} T\underset{0\le\tau\le T}{max}|a(\tau)|\left(\sum_{n=1}^{\infty}\left(\lambda_n^{5/2}\underset{0\le\tau\le T}{max}|z_n(\tau)|\right)^2\right)^{1/2}\Bigg]. \end{aligned} \quad (21)$$

Since the right hand side of (21) is bounded, $\theta_2(w) \in C[0,T]$. Thus Θ maps E_T^5 onto itself continuously.

Let us now show that Θ is a contraction mapping on E_T . Let us choose any two elements $w_i = \left[z^i(\kappa,\tau), a^i(\tau)\right]^T$, $i = 1,2$ in E_T. We know that $\|\Theta(w_1) - \Theta(w_2)\|_{E_T} =$.

Under the assumptions $(A_1) - (A_3)$ and considering (20)-(21), we obtain

$$\|\Theta(w_1) - \Theta(w_2)\|_{E_T} \le A(T)\,\|w_1 - w_2\|_{E_T}$$

where

$$A(T) = T\widehat{C}\left\{1 + \frac{1}{\underset{0\le\tau\le T}{min}|r(\tau)|}\left(\sum_{n=1}^{\infty}\frac{1}{\lambda_n^3}\right)^{1/2}\right\} D(a^1, z^2)$$

and $D(a^1, z^2) = \max\left\{\left\|a^1(\tau)\right\|_{C[0,T]}, \left\|z^2(\kappa,\tau)\right\|_{B_T}\right\}$.

It can be seen that $\lim A(T) \to 0$ as $T \to 0$. Thus the operator Θ is contraction mapping which maps E_T onto itself continuously for sufficient small times. Then there exists a unique solution of (15) by virtue of the Banach fixed point theorem. Thus, the problem (1)-(4) has a unique solution for small T. □

5. Numerical approach of the direct problem

In this section, first we do the time discretization of the direct problem (1) using backward Euler formulation. Let us slice the temporal domain $[0,T]$ into N subintervals of equal length $\Delta\tau = \frac{T}{N}$ using the knots $0 = \tau_0, \tau_1, \cdots, \tau_N = T$, where $\tau_n = n \times \Delta\tau$ for $n = 0 : 1 : N$. At a certain time level $\tau = \tau_{n+1}$, the Caputo time fractional derivative can be discretized as [1]

$$\begin{aligned}\frac{\partial^\alpha}{\partial\tau^\alpha}z(\kappa,\tau_{n+1}) =& \frac{1}{\Gamma(1-\alpha)}\int_0^{\tau_{y+1}}\frac{\partial}{\partial y}z(\kappa,y)\times(\tau_{n+1}-y)^{-\alpha}dy \\ =& \frac{1}{\Gamma(1-\alpha)}\sum_{r=0}^{n}\int_{\tau_r}^{\tau_{r+1}}\frac{\partial}{\partial y}z(\kappa,y)\times(\tau_{n+1}-y)^{-\alpha}dy \\ =& \frac{1}{\Gamma(1-\alpha)}\sum_{r=0}^{n}\frac{z(\kappa,\tau_{n+1})-z(\kappa,\tau_n)}{\Delta\tau}\times\int_{\tau_r}^{\tau_{r+1}}(\tau_{n+1}-y)^{-\alpha}dy + E_{\Delta\tau}^{n+1}\end{aligned}$$

$$=\frac{1}{\Gamma(1-\alpha)}\sum_{r=0}^{n}\frac{z(\kappa,\tau_{n+1})-z(\kappa,\tau_n)}{\Delta\tau}\times\int\limits_{\tau_{n-r}}^{\tau_{n-r+1}}x^{-\alpha}dx+E_{\Delta\tau}^{n+1}$$

$$=\frac{1}{\Gamma(1-\alpha)}\sum_{r=0}^{n}\frac{z(\kappa,\tau_{n-r+1})-z(\kappa,\tau_{n-r})}{\Delta\tau}\times\int\limits_{\tau_{r}}^{\tau_{r+1}}x^{-\alpha}dx+E_{\Delta\tau}^{n+1}$$

$$=\frac{1}{\Gamma(2-\alpha)}\sum_{r=0}^{n}\omega_r\frac{z(\kappa,\tau_{n-r+1})-z(\kappa,\tau_{n-r})}{\Delta\tau^{\alpha}}+E_{\Delta\tau}^{n+1}, \tag{22}$$

where

$x=\tau_{n+1}-y,\quad \omega_r=(r+1)^{1-\alpha}-(r)^{1-\alpha},\quad |E_{\Delta\tau}^{n+1}|\leq \digamma\Delta\tau^{2-\alpha}, \digamma$ is a finite constant,
$\omega_r\geq 0,\ \forall r,\quad 1=\omega_0>\omega_1>\omega_2>\omega_3>\cdots>\omega_n,\ \omega_n\to 0$ as $n\to\infty$,
$\sum_{r=0}^{n}(\omega_r-\omega_{r+1})+\omega_{n+1}=(\omega_0-\omega_1)+\sum_{r=1}^{n-1}(\omega_r-\omega_{r+1})+\omega_n=1.$

Hence,

$$\frac{\partial^{\alpha}}{\partial\tau^{\alpha}}z(\kappa,\tau_{n+1})=\frac{1}{\Gamma(2-\alpha)}\sum_{r=0}^{n}\omega_r\frac{z(\kappa,\tau_{n-r+1})-z(\kappa,\tau_{n-r})}{\Delta\tau^{\alpha}}. \tag{23}$$

Using (23) and Crank-Nicolson scheme in equation (1), we get

$$\frac{\Delta\tau^{-\alpha}}{\Gamma(2-\alpha)}\sum_{r=0}^{n}\omega_r\Big[z(\kappa,\tau_{n-r+1})-z(\kappa,\tau_{n-r})\Big]-\Big[\frac{z_{\kappa\kappa}(\kappa,\tau_{n+1})-z_{\kappa\kappa}(\kappa,\tau_n)}{\Delta\tau}\Big]$$
$$=\frac{1}{2}\Big[a(\tau_{n+1})z(\kappa,\tau_{n+1})+a(\tau_n)z(\kappa,\tau_n)\Big]+\frac{1}{2}\Big[f(\kappa,\tau_{n+1})+f(\kappa,\tau_n)\Big],$$
$$n=0,1,2,\cdots,N-1. \tag{24}$$

After some simplification, the last equation is reshaped as

$$2\eta\omega_0 z(\kappa,\tau_{n+1})-\frac{2}{\Delta\tau}\Big[z_{\kappa\kappa}(\kappa,\tau_{n+1})\Big]-a(\tau_{n+1})z(\kappa,\tau_{n+1})=2\eta\omega_0 z(\kappa,\tau_n)$$
$$-\frac{2}{\Delta\tau}\Big[z_{\kappa\kappa}(\kappa,\tau_n)\Big]+a(\tau_n)z(\kappa,\tau_n)+f(\kappa,\tau_{n+1})+f(\kappa,\tau_n)$$
$$-2\eta\sum_{r=1}^{n}\omega_r\Big[z(\kappa,\tau_{n-r+1})-z(\kappa,\tau_{n-r})\Big], \tag{25}$$

where $\eta=\frac{\Delta\tau^{-\alpha}}{\Gamma(2-\alpha)}$. Now, we discretize the problem in spatial direction by defining a uniform partition of the space interval $[0,\ell]$ with $M+1$ equidistant knots $0=\kappa_0,\kappa_1,\cdots,\kappa_M=\ell$ such that $\kappa_m=m\times\Delta\kappa$ where $\Delta\kappa=\frac{\ell}{M}$ and $m=0:1:M$. Let the approximate solution for the proposed problem in terms of cubic B-spline functions is given by

$$Z(\kappa,\tau_{n+1})=\sum_{p=-1}^{m+1}\sigma_p(\tau_{n+1})Q_p(\kappa), \tag{26}$$

where σ_p's are time dependant control points and $Q_p(\kappa)$, $p = -1, 0, \cdots, m+1$, are the typical cubic B-spline functions defined as [13]

$$Q_p(\kappa) = \frac{1}{6\Delta\kappa^3}\begin{cases} (\kappa-\kappa_{p-2})^3, & \kappa \in [\kappa_{p-2}, \kappa_{p-1}], \\ \Delta\kappa^3 - 3\Delta\kappa^2(\kappa_{p-1}-\kappa) + 3\Delta\kappa(\kappa_{p-1}-\kappa)^2 + 3(\kappa_{p-1}-\kappa)^3, & \kappa \in [\kappa_{p-1}, \kappa_p], \\ \Delta\kappa^3 - 3\Delta\kappa^2(\kappa-\kappa_{p+1}) + 3\Delta\kappa(\kappa-\kappa_{p+1})^2 + 3(\kappa-\kappa_{p+1})^3, & \kappa \in [\kappa_p, \kappa_{p+1}], \\ (\kappa_{p+2}-\kappa)^3, & \kappa \in [\kappa_{p+1}, \kappa_{p+2}], \\ 0, & \text{otherwise.} \end{cases} \tag{27}$$

Using (26) in equation (25), we get

$$\begin{aligned} 2\eta\omega_0 Z(\kappa, \tau_{n+1}) - \frac{2}{\Delta\tau}\Big[Z_{\kappa\kappa}(\kappa, \tau_{n+1})\Big] - a(\tau_{n+1})Z(\kappa, \tau_{n+1}) = 2\eta\omega_0 Z(\kappa, \tau_n) \\ - \frac{2}{\Delta\tau}\Big[Z_{\kappa\kappa}(\kappa, \tau_n)\Big] + a(\tau_n)Z(\kappa, \tau_n) + f(\kappa, \tau_{n+1}) + f(\kappa, \tau_n) \\ - 2\eta\sum_{r=1}^{n}\omega_r\Big[Z(\kappa, \tau_{n-r+1}) - Z(\kappa, \tau_{n-r})\Big]. \end{aligned} \tag{28}$$

Discretizing the last equation at $\kappa = \kappa_m$, we obtain

$$\begin{aligned} 2\eta\omega_0 Z(\kappa_m, \tau_{n+1}) - \frac{2}{\Delta\tau}\Big[Z_{\kappa\kappa}(\kappa_m, \tau_{n+1})\Big] - a(\tau_{n+1})Z(\kappa_m, \tau_{n+1}) = 2\eta\omega_0 Z(\kappa_m, \tau_n) \\ - \frac{2}{\Delta\tau}\Big[Z_{\kappa\kappa}(\kappa_m, \tau_n)\Big] + a(\tau_n)Z(\kappa_m, \tau_n) + f(\kappa_m, \tau_{n+1}) + f(\kappa_m, \tau_n) \\ - 2\eta\sum_{r=1}^{n}\omega_r\Big[Z(\kappa_m, \tau_{n-r+1}) - Z(\kappa_m, \tau_{n-r})\Big], \quad m = 0, 1, \cdots, M. \end{aligned} \tag{29}$$

For the sake of simplicity, we denote $Z(\kappa_m, \tau_n) = Z_m^n$, $a(\tau_n) = a^n$ and $f(\kappa_m, \tau_n) = f_m^n$ to reshape equation (29) as

$$\begin{aligned} 2\eta\omega_0 Z_m^{n+1} - \frac{2}{\Delta\tau}(Z_{\kappa\kappa})_m^{n+1} - a^{n+1}Z_m^{n+1} = 2\eta\omega_0 Z_m^n - \frac{2}{\Delta\tau}(Z_{\kappa\kappa})_m^n \\ + a^n Z_m^n + f_m^{n+1} + f_m^n - 2\eta\sum_{r=1}^{n}\omega_r\Big[Z_m^{n-r+1} - Z_m^{n-r}\Big], \quad m = 0, 1, \cdots, M. \end{aligned} \tag{30}$$

Using (26) and (27), we obtain the following relations

$$Z_m^n = \frac{1}{6}(\sigma_{m-1}^n + 4\sigma_m^n + \sigma_{m-1}^n), \tag{31}$$

$$(Z_\kappa)_m^n = \frac{1}{2\Delta\kappa}(-\sigma_{m-1}^n + \sigma_{m+1}^n), \tag{32}$$

$$(Z_{\kappa\kappa})_m^n = \frac{1}{\Delta\kappa^2}(\sigma_{m-1}^n - 2\sigma_m^n + \sigma_{m+1}^n). \tag{33}$$

Now, substituting (31) and (33) into (30), we get

$$\begin{aligned}
&\frac{\eta\omega_0}{3}(\sigma_{m-1}^{n+1}+4\sigma_m^{n+1}+\sigma_{m-1}^{n+1})-\frac{2}{\Delta\tau\Delta\kappa^2}(\sigma_{m-1}^{n+1}-2\sigma_m^{n+1}+\sigma_{m+1}^{n+1})\\
&\quad-\frac{a^{n+1}}{6}(\sigma_{m-1}^{n+1}+4\sigma_m^{n+1}+\sigma_{m-1}^{n+1})=\frac{\eta\omega_0}{3}(\sigma_{m-1}^{n}+4\sigma_m^{n}+\sigma_{m-1}^{n})\\
&\quad-\frac{2}{\Delta\tau\Delta\kappa^2}(\sigma_{m-1}^{n}-2\sigma_m^{n}+\sigma_{m+1}^{n})+\frac{a^n}{6}(\sigma_{m-1}^{n}+4\sigma_m^{n}+\sigma_{m-1}^{n})\\
&-\frac{\eta}{3}\sum_{r=1}^{n}\omega_r\Big[(\sigma_{m-1}^{n-r+1}+4\sigma_m^{n-r+1}+\sigma_{m-1}^{n-r+1})-(\sigma_{m-1}^{n-r}+4\sigma_m^{n-r}+\sigma_{m-1}^{n-r})\Big]+F_m^{n+1},\\
&\qquad\qquad m=0,1,\cdots,M, \quad (34)
\end{aligned}$$

where $F_m^{n+1}=f_m^{n+1}+f_m^n$. The expression (34) represents $M+1$ equations involving $M+3$ unknown control points at $\tau=\tau_{n+1}, n=0,1,\cdots,N-1$. In order to obtain a unique solution to the problem, two more equations are extracted from the given boundary conditions (3) as

$$\sigma_{-1}^{n+1}+4\sigma_0^{n+1}+\sigma_1^{n+1}=0, \tag{35}$$

$$\sigma_{M-1}^{n+1}+4\sigma_M^{n+1}+\sigma_{M+1}^{n+1}=0. \tag{36}$$

The set of equations (34)–(36) can be written in matrix form as

$$L_1\sigma^{n+1}=L_2\sigma^n-L_3\sum_{r=1}^{n}\frac{\eta\omega_r}{3}\Big(\sigma^{n-r+1}-\sigma^{n-r}\Big)+\Psi^{n+1}, \quad n=0,1,\cdots,N-1, \tag{37}$$

where

$$L_1=\begin{pmatrix}
1 & 4 & 1 & 0 & \cdots & 0 & 0 & 0 & 0\\
l_1 & l_2 & l_1 & 0 & \cdots & 0 & 0 & 0 & 0\\
0 & l_1 & l_2 & l_1 & \cdots & 0 & 0 & 0 & 0\\
\vdots & \ddots & \ddots & \ddots & & \ddots & \ddots & \ddots & \vdots\\
0 & 0 & 0 & 0 & \cdots & l_1 & l_2 & l_1 & 0\\
0 & 0 & 0 & 0 & \cdots & 0 & l_1 & l_2 & l_1\\
0 & 0 & 0 & 0 & \cdots & & 1 & 4 & 1
\end{pmatrix},$$

$$L_2=\begin{pmatrix}
0 & 0 & 0 & 0 & \cdots & 0 & 0 & 0 & 0\\
l_3 & l_4 & l_3 & 0 & \cdots & 0 & 0 & 0 & 0\\
0 & l_3 & l_4 & l_3 & \cdots & 0 & 0 & 0 & 0\\
\vdots & \ddots & \ddots & \ddots & & \ddots & \ddots & \ddots & \vdots\\
0 & 0 & 0 & 0 & \cdots & l_3 & l_4 & l_3 & 0\\
0 & 0 & 0 & 0 & \cdots & 0 & l_3 & l_4 & l_3\\
0 & 0 & 0 & 0 & \cdots & & 0 & 0 & 0
\end{pmatrix},$$

$$L_3 = \begin{pmatrix} 0 & 0 & 0 & 0 & \cdots & 0 & 0 & 0 & 0 \\ l_5 & l_6 & l_5 & 0 & \cdots & 0 & 0 & 0 & 0 \\ 0 & l_5 & l_6 & l_5 & \cdots & 0 & 0 & 0 & 0 \\ \vdots & \ddots & \ddots & \ddots & \ddots & \ddots & \ddots & \ddots & \vdots \\ 0 & 0 & 0 & 0 & \cdots & l_5 & l_6 & l_5 & 0 \\ 0 & 0 & 0 & 0 & \cdots & 0 & l_5 & l_6 & l_5 \\ 0 & 0 & 0 & 0 & \cdots & 0 & 0 & 0 & 0 \end{pmatrix},$$

$$\sigma^n = \begin{pmatrix} \sigma^n_{-1} \\ \sigma^n_0 \\ \sigma^n_1 \\ \vdots \\ \sigma^n_{M-1} \\ \sigma^n_M \\ \sigma^n_{M+1} \end{pmatrix}, \quad \Psi^{n+1} = \begin{pmatrix} f_0^{n+1} + f_0^n \\ f_1^{n+1} + f_1^n \\ f_2^{n+1} + f_2^n \\ \vdots \\ f_{M-2}^{n+1} + f_{M-2}^n \\ f_{M-1}^{n+1} + f_{M-1}^n \\ f_M^{n+1} + f_M^n \end{pmatrix},$$

$$l_1 = -\frac{a^{n+1}}{6} - \frac{2}{\Delta\tau\Delta\kappa^2} + \frac{\eta}{3}, \quad l_2 = -\frac{2a^{n+1}}{3} + \frac{4}{\Delta\tau\Delta\kappa^2} + \frac{4\eta}{3},$$
$$l_3 = \frac{a^{n+1}}{6} - \frac{2}{\Delta\tau\Delta\kappa^2} + \frac{\eta}{3}, \quad l_4 = \frac{2a^{n+1}}{3} + \frac{4}{\Delta\tau\Delta\kappa^2} + \frac{4\eta}{3}, \quad l_5 = 1, \quad l_6 = 4.$$

The system of equations (37) is solved for $\sigma_{-1}, \cdots, \sigma_{m+1}$ and their values are plugged into equation (26) to get the approximate solution at $\tau = \tau_{n+1}, n = 0, 1, \cdots, N-1$. However, before starting any computation using (37), the control points at the initial time level are to be determined. For this, the following system of equations is obtained from the given initial condition (2)

$$\begin{cases} -\sigma^0_{-1} + \sigma^0_1 = 2\Delta\kappa(\xi_\kappa)^0_0, \\ \sigma^0_{m-1} + 4\sigma^0_m + \sigma^0_{m+1} = 6\xi^0_m, \qquad m = 0, 1, \cdots, M, \\ -\sigma^0_{M-1} + \sigma^0_{M+1} = 2\Delta\kappa(\xi_\kappa)^0_M. \end{cases} \tag{38}$$

The system of equations (38) is solved by using a modified from of Thomas algorithm to get the required set of control points at initial time level.

6. Stability analysis of the proposed numerical scheme

In this section, we examine the stability of the direct numerical scheme using Fourier method [3]. For this, let us take the full discretized form of the equation (1)

$$2\eta Z_m^{n+1} - \frac{2}{\Delta\tau}(Z_{\kappa\kappa})_m^{n+1} - a^{n+1}Z_m^{n+1} = 2\eta Z_m^n - \frac{2}{\Delta\tau}(Z_{\kappa\kappa})_m^n + a^n Z_m^n + f_m^{n+1} + f_m^n$$
$$- 2\eta\sum_{r=1}^{n}\omega_r\Big[Z_m^{n-r+1} - Z_m^{n-r}\Big],\ m = 0, 1, \cdots, M,\ n = 0, 1, \cdots, N-1. \quad (39)$$

Let $\mho^n$ and $\tilde{\mho}^n$ be the exact and approximate values of the growth factor in Fourier mode. Then the error at $\tau = \tau_n$ is given by

$$\aleph^n = \mho^n - \tilde{\mho}^n, \quad (40)$$

where $\aleph^n = [\aleph_1^n, \aleph_2^n, \aleph_3^n, \cdots, \aleph_{N-1}^n]^T$. Now, using (39) and (40), the following error equation is obtained

$$l_1\aleph_{m-1}^{n+1} + l_2\aleph_m^{n+1} + l_1\aleph_{m+1}^{n+1} = l_3\aleph_{m-1}^n + l_4\aleph_m^n + l_3\aleph_{m+1}^n$$
$$- \frac{\eta}{3}\sum_{r=1}^{n}\omega_r\Big[l_5(\aleph_{m-1}^{n-r+1} - \aleph_{m-1}^{n-r}) + l_6(\aleph_m^{n-r+1} - \aleph_m^{n-r}) + l_5(\aleph_{m+1}^{n-r+1} - \aleph_{m+1}^{n-r})\Big]. \quad (41)$$

Moreover, the initial and the boundary conditions are satisfied by the error equation. Now, we introduce the mesh function in Fourier form as

$$\aleph^n = \begin{cases} \aleph_m^n, & \kappa_m - \frac{\Delta\kappa}{2} < \kappa \le \kappa_m + \frac{\Delta\kappa}{2},\ m = 1:1:M-1, \\ 0, & 0 \le \kappa \le \frac{\Delta\kappa}{2}\ or\ \ell - \frac{\Delta\kappa}{2} \le \kappa \le \ell. \end{cases} \quad (42)$$

Hence, $\aleph^n(\kappa)$ in terms of Fourier series is given by

$$\aleph^n(\kappa) = \sum_{-\infty}^{\infty}\varsigma_n(m)e^{\frac{2i\pi m\kappa}{\ell}}, \quad n = 0:1:N, \quad (43)$$

where

$$\varsigma_n(m) = \frac{1}{\ell}\int_0^\ell \aleph^n(\kappa)e^{\frac{-2i\pi m\kappa}{\ell}}d\kappa.$$

By applying norm, we get

$$\|\aleph^n\|_2 = \sqrt{\sum_{m=1}^{M-1}\Delta\kappa|\aleph_m^n|^2}$$
$$= \sqrt{\int_0^{\frac{\Delta\kappa}{2}}|\aleph^n|^2 d\kappa + \sum_{m=1}^{M-1}\int_{\kappa_m-\frac{\Delta\kappa}{2}}^{\kappa_m+\frac{\Delta\kappa}{2}}|\aleph^n|^2 d\kappa + \int_{\ell-\frac{\Delta\kappa}{2}}^{\ell}|\aleph^n|^2 d\kappa},$$
$$\|\aleph^n\|_2^2 = \int_0^\ell |\aleph^n|^2 d\kappa.$$

Hence, by using the Parseval's equality [15]

$$\|\aleph^n\|_2^2 = \sum_{-\infty}^{\infty}|\varsigma_n(m)|^2. \quad (44)$$

Now, we substitute $\aleph_m^n = \varsigma_n e^{i\gamma m \Delta\kappa}$ into equation (41)

$$l_1\varsigma_{n+1}e^{i\gamma(m-1)\Delta\kappa}+l_2\varsigma_{n+1}e^{i\gamma m\Delta\kappa}+l_1\varsigma_{n+1}e^{i\gamma(m+1)\Delta\kappa} = l_3\varsigma_n e^{i\gamma(m-1)\Delta\kappa}+l_4\varsigma_n e^{i\gamma m\Delta\kappa}$$
$$+l_3\varsigma_n e^{i\gamma(m+1)\Delta\kappa}-\frac{\eta}{3}\sum_{r=1}^{n}\omega_r\Big[l_5(\varsigma_{n-r+1}e^{i\gamma(m-1)\Delta\kappa}-\varsigma_{n-r}e^{i\gamma(m-1)\Delta\kappa})+l_6(\varsigma_{n-r+1}e^{i\gamma m\Delta\kappa}$$
$$-\varsigma_{n-r}e^{i\gamma m\Delta\kappa})+l_5(\varsigma_{n-r+1}e^{i\gamma(m+1)\Delta\kappa}-\varsigma_{n-r}e^{i\gamma(m+1)\Delta\kappa})\Big], \quad (45)$$

where $i=\sqrt{-1}$ and $\gamma = \frac{2\pi m}{\ell}$.
After simplification, the last equation takes the following form

$$\Big[2l_1\cos(\gamma\Delta\kappa)+l_2\Big]\varsigma_{n+1} = \Big[2l_3\cos(\gamma\Delta\kappa)+l_4\Big]\varsigma_n$$
$$-\frac{\eta}{3}\sum_{r=1}^{n}\omega_r\Big[\Big\{2l_5\cos(\gamma\Delta\kappa)+l_6\Big\}(\varsigma_{n-r+1}-\varsigma_{n-r})\Big]. \quad (46)$$

Hence,

$$\varsigma_{n+1} = \frac{a_2}{a_1}\varsigma_n + \frac{1}{a_1}\sum_{r=1}^{n}\omega_r\Big[\varsigma_{n-r}-\varsigma_{n-r+1}\Big], \quad (47)$$

where

$$a_1 = 2+\frac{24\sin^2(\Delta\kappa\gamma/2)-2a_{n+1}\Delta\kappa^2\Delta\tau(1+2\cos^2(\Delta\kappa\gamma/2))}{\eta\Delta\kappa^2\Delta\tau(1+2\cos^2(\Delta\kappa\gamma/2)))},$$
$$a_2 = 2+\frac{24\sin^2(\Delta\kappa\gamma/2)+2a_n\Delta\kappa^2\Delta\tau(1+2\cos^2(\Delta\kappa\gamma/2))}{\eta\Delta\kappa^2\Delta\tau(1+2\cos^2(\Delta\kappa\gamma/2)))}.$$

We use mathematical induction to prove that $|\varsigma_n|\le|\varsigma_0|$, for all n. For $n=0$, equation (47) takes the following form

$$|\varsigma_1| = \frac{a_2}{a_1}|\varsigma_0| \le |\varsigma_0|, \quad \because a_1 \ge a_2.$$

Now, assuming that the required result is true for $n=k>1$, i.e. $|\varsigma_k|\le|\varsigma_0|$, we proceed as

$$|\varsigma_{k+1}| \le \frac{a_2}{a_1}|\varsigma_k| + \frac{1}{a_1}\sum_{r=1}^{n}\omega_r\Big[|\varsigma_{k-r}|-|\varsigma_{k-r+1}|\Big]$$
$$\le \frac{a_2}{a_1}|\varsigma_0| + \frac{1}{a_1}\sum_{r=1}^{n}\omega_r\Big[|\varsigma_0|-|\varsigma_0|\Big]$$
$$\le |\varsigma_0|.$$

Hence,

$$|\varsigma_k|\le|\varsigma_0| \quad \text{for all } n. \quad (48)$$

Consequently, from (44) and (48), we have

$$\|\aleph^n\|_2 \le \|\aleph^0\|_2, \quad \forall\, n = 0,1,2,\cdots,N.$$

Hence, the proposed scheme is numerically stable.

Example: Consider the following example of the direct problem (1)–(3) with $\ell = T = 1$:

$$\frac{\partial^\alpha z(\kappa,\tau)}{\partial\tau^\alpha} - \frac{\partial^3 z(\kappa,\tau)}{\partial\kappa^2\partial\tau} = a(\tau)z(\kappa,\tau) + f(\kappa,\tau), \quad \kappa \in [0,1], \quad \tau \in [0,1],$$

where $a(\tau) = -1 - 2\tau$, with

$$\xi(\kappa) = z(\kappa,0) = \sin(\pi\kappa), \quad \kappa \in [0,1], \tag{49}$$

and

$$z(0,\tau) = z(1,\tau) = 0, \quad \tau \in [0,1],$$

where

$$f(\kappa,\tau) = \frac{\sin(\pi\kappa)\left(-\pi^2 - \tau^{1-\alpha}\right)}{\Gamma(2-\alpha) + (\tau-1)(-1-2\tau)\sin(\pi\kappa)}, \quad \alpha \in (0,1). \tag{50}$$

The analytical exact solution is

$$z(\kappa,\tau) = \sin(\pi\kappa)(1-\tau), \quad (\kappa,\tau) \in [0,1] \times [0,1]. \tag{51}$$

Tables 1, 2 and 3 show the absolute errors for different choices of α setting $M = N = 20, 40, 80$ and $\tau = 0.9$. From these tables, we can see that the absolute errors are reduced as the mesh sizes are decreased. Figures 1, 2 and 3 depict the numerical temperature in comparison of the exact (51) at $\tau = 1$ with $M = N = 50, 100$, and $\alpha \in (0.1, 0.5, 0.9)$ obtained by using the CB-spline collocation method as described in Section 5. From these figures, we can observe that an excellent agreement between the approximate and exact solutions is obtained.

TABLE 1. The absolute errors between the approximate and analytical (51) solutions for $z(\kappa,\tau)$ with various choices of α, where $M = N = 20$ at $\tau = 0.9$.

κ	Error $\alpha = 0.2$	Error $\alpha = 0.5$	Error $\alpha = 0.9$
0.1	1.100E-3	1.200E-3	1.100E-3
0.2	2.200E-3	2.200E-3	2.100E-3
0.3	3.000E-3	3.100E-3	2.900E-3
0.4	3.500E-3	3.600E-3	3.400E-3
0.5	3.700E-3	3.800E-3	3.600E-3
0.6	3.500E-3	3.600E-3	3.400E-3
0.7	3.000E-3	3.100E-3	2.900E-3
0.8	2.200E-3	2.200E-3	2.100E-3
0.9	1.100E-3	1.200E-3	1.100E-3

TABLE 2. The absolute errors between the approximate and analytical (51) solutions for $z(\kappa,\tau)$ with various choices of α, where $M = N = 40$ at $\tau = 0.9$.

κ	Error $\alpha = 0.2$	Error $\alpha = 0.5$	Error $\alpha = 0.9$
0.1	4.495E-4	4.626E-4	4.371E-4
0.2	8.550E-4	8.799E-4	8.315E-4
0.3	1.200E-3	1.200E-3	1.100E-3
0.4	1.400E-3	1.400E-3	1.300E-3
0.5	1.500E-3	1.500E-3	1.400E-3
0.6	1.400E-3	1.400E-3	1.300E-3
0.7	1.200E-3	1.200E-3	1.100E-3
0.8	8.550E-4	8.799E-4	8.315E-4
0.9	4.495E-4	4.626E-4	4.371E-4

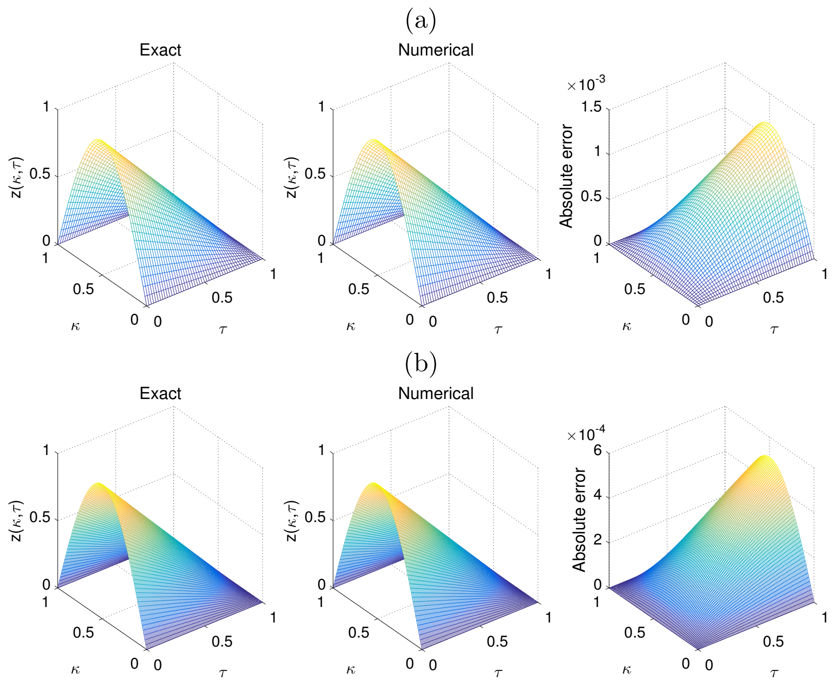

FIGURE 1. The numerical and exact (51) solutions for $z(\kappa,\tau)$, and the absolute computational error between them, with $\alpha = 0.1$ at $\tau = 1$ for: (a) $M = N = 50$ and (b) $M = N = 100$, for the forward problem.

TABLE 3. The absolute errors between the approximate and analytical (51) solutions for $z(\kappa,\tau)$ with various choices of α, where $M = N = 80$ at $\tau = 0.9$.

κ	Error $\alpha = 0.2$	Error $\alpha = 0.5$	Error $\alpha = 0.9$
0.1	1.942E-4	2.011E-4	1.888E-4
0.2	3.694E-4	3.826E-4	3.591E-4
0.3	5.085E-4	5.267E-4	4.943E-4
0.4	5.978E-4	6.192E-4	5.811E-4
0.5	6.286E-4	6.510E-4	6.110E-4
0.6	5.978E-4	6.192E-4	5.811E-4
0.7	5.085E-4	5.267E-4	4.943E-4
0.8	3.694E-4	3.826E-4	3.591E-4
0.9	1.942E-4	2.011E-4	1.888E-4

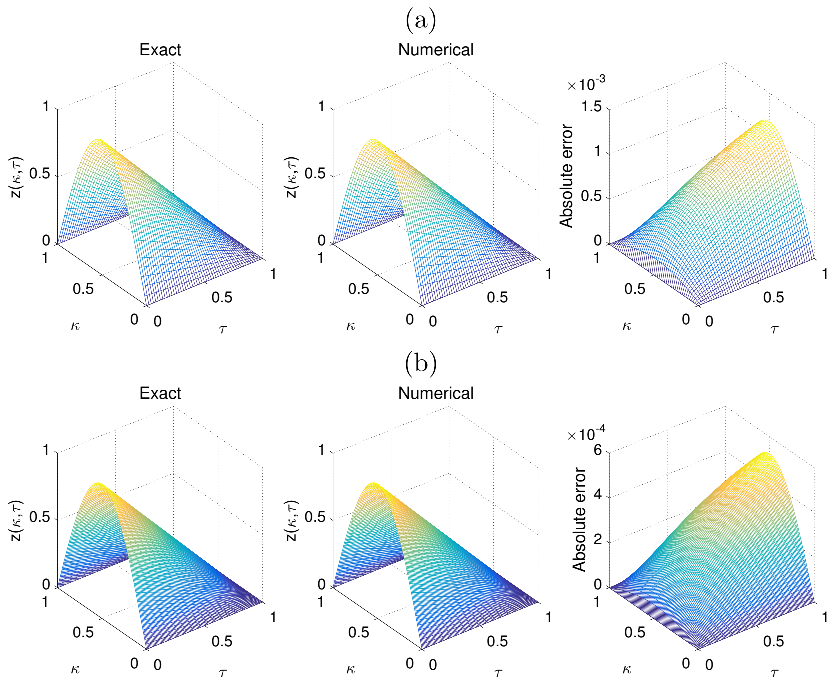

FIGURE 2. The numerical and exact (51) solutions for $z(\kappa,\tau)$, and the absolute computational error between them, with $\alpha = 0.5$ at $\tau = 1$ for: (a) $M = N = 50$ and (b) $M = N = 100$, for the forward problem.

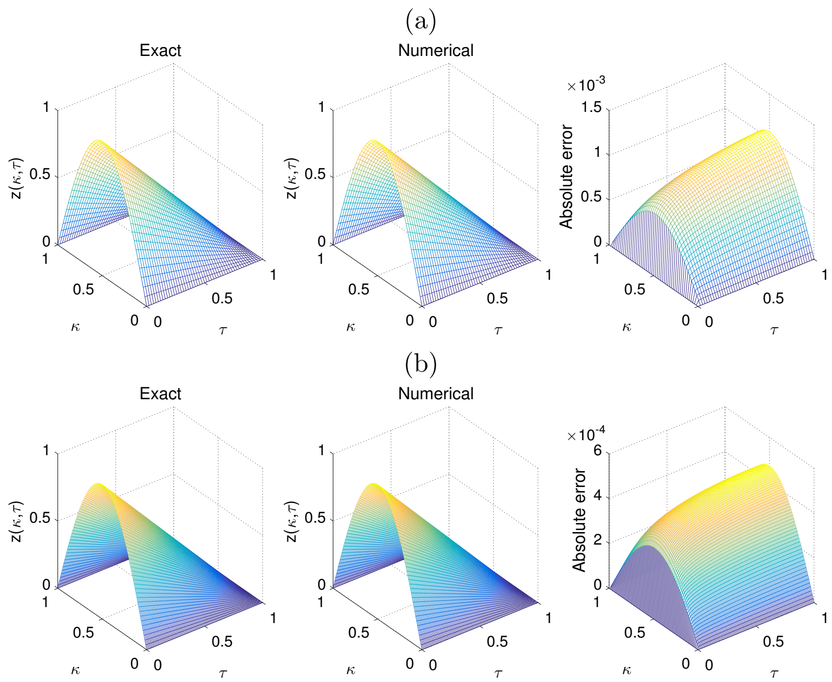

FIGURE 3. The numerical and exact (51) solutions for $z(\kappa,\tau)$, and the absolute computational error between them, with $\alpha = 0.9$ at $\tau = 1$ for: (a) $M = N = 50$ and (b) $M = N = 100$, for the forward problem.

7. Numerical approach of the inverse problem

We want to get accurate and stable determinations of $a(\tau)$ and $z(\kappa,\tau)$ that satisfy (1)–(4). The proposed problem is numerically solved by minimizing the following regularized cost function

$$F(a) = \delta||a(\tau)||^2 + \|z(X_0,\tau) - r(\tau)\|^2 \, , \tag{52}$$

where z satisfies the forward problem (1)-(3) with given $a(\tau)$, and δ is the non-negative penalty parameter. The discretized form of above function is given by

$$F(\underline{a}) = \sum_{n=1}^{N} [z(X_0,\tau_n) - r(\tau_n)]^2 + \delta \sum_{n=1}^{N} (a^n)^2. \tag{53}$$

The cost function (53) is minimizing by means of the MATLAB subroutine *lsqnonlin* tool [18].

8. Numerical results and discussion

A couple of experiment examples have been discussed in this section to demonstrate the stability and accuracy of the CB-spline technique together with the Tikhonov regularization process. To validate the efficeincy of the approximate solution, the RMSE has been calculated as:

$$\text{RMSE}(a) = \left[\frac{T}{N} \sum_{n=1}^{N} \left(a^{numerical}(\tau_n) - a^{exact}(\tau_n) \right)^2 \right]^{1/2}. \tag{54}$$

For the sake of simplicity, we set $\ell = T = 1$. The upper and lower bounds for $a(\tau)$ are supposed to be 10^2 and -10^2, respectively.

The problem (1)–(4) has been solved with both perturbed and exact data. The perturbed data is handled as

$$r^{\epsilon}(\tau_n) = r(\tau_n) + \epsilon_n, \quad n = 1, 2, ..., N, \tag{55}$$

where ϵ_n's denote the random variables and the following S.D.s

$$\sigma = \max_{0 \le \tau \le T} |r(\tau)| \times p. \tag{56}$$

For the perturbed data (55), $r(\tau_n)$ is replaced by $r^{\epsilon}(\tau_n)$ in (53).

8.1. Example 1. As a first test problem, we take (1)–(4) with input (49)–(51), and the unknown smooth and linear time-dependent term $a(\tau)$

$$a(\tau) = -1 - 2\tau, \quad \tau \in [0, 1], \tag{57}$$

and the target output (4) is

$$r(\tau) = z(X_0, \tau) = 1 - \tau, \quad X_0 = 0.5, \quad \tau \in [0, 1]. \tag{58}$$

Tables 4 and 5 show the absolute errors between the approximate and exact (58) solutions for $r(\tau)$ with different choices of α and τ, using different values of M and N at $\kappa = 0$.

Table 4. Absolute errors between the approximate and analytical (58) solutions for $r(\tau)$, with various choices of α, where $M = N = 40$ at $\kappa = 0$.

τ	Error $\alpha = 0.1$	Error $\alpha = 0.3$	Error $\alpha = 0.9$
0.1	3.3823E-5	5.0885E-5	1.6034E-4
0.2	6.3333E-5	8.4251E-5	1.7594E-4
0.3	9.0847E-5	1.1271E-4	1.8707E-4
0.4	1.1675E-4	1.3801E-4	1.9600E-4
0.5	1.4119E-4	1.6086E-4	2.0349E-4
0.6	1.6423E-4	1.8166E-4	2.0984E-4
0.7	1.8590E-4	2.0063E-4	2.1526E-4
0.8	2.0621E-4	2.1791E-4	2.1985E-4
0.9	2.2517E-4	2.3363E-4	2.2368E-4

TABLE 5. Absolute errors between the approximate and analytical (58) solutions for $r(\tau)$, with various choices of α, where $M = N = 80$ at $\kappa = 0$.

τ	Error $\alpha = 0.1$	Error $\alpha = 0.3$	Error $\alpha = 0.9$
0.1	1.0554E-5	1.6607E-5	5.5370E-5
0.2	1.9617E-5	2.7049E-5	5.9589E-5
0.3	2.8013E-5	3.5793E-5	6.2255E-5
0.4	3.5882E-5	4.3461E-5	6.4176E-5
0.5	4.3280E-5	5.0311E-5	6.5614E-5
0.6	5.0232E-5	5.6480E-5	6.6692E-5
0.7	5.6752E-5	6.2052E-5	6.7476E-5
0.8	6.2847E-5	6.7082E-5	6.8008E-5
0.9	6.8522E-5	7.1611E-5	6.8319E-5

From given data it can be observed that the conditions of Theorem 4.1 are satisfied, so, the problem possesses a unique solution. The initial approximation for the vector $\underline{a}$ is taken as

$$a^0(\tau_n) = a(0) = -1, \quad n = 1, 2, ..., N. \tag{59}$$

For the inverse problem, we use $\Delta\kappa = \Delta\tau = 0.025$ and $\alpha = 0.5$. In Figure 4(a), the unregularized function (53), i.e. $\delta = 0$ has been plotted versus number of iterations in absence of noise in measurement data. It can be noted that after nine iterations, there is a quick decline low value of $O(10^{-16})$. The approximate and exact solutions to the function $a(\tau)$ are portrayed in Figure 4(b). It is observed that the numerical outcomes are very accurate with a RMSE(a) =0.0693.

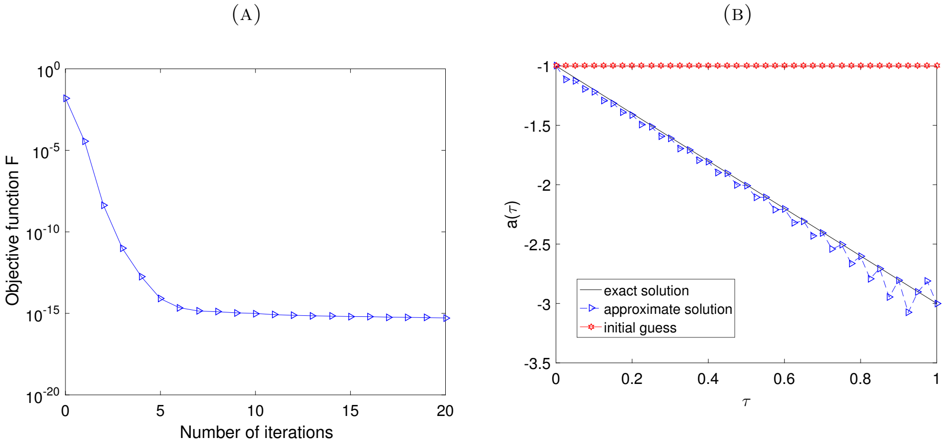

FIGURE 4. (a) The unregularized form of cost function F (53) versus no. of iterations, (b) the approximate and analytical exact curves for the potential term $a(\tau)$, in absence of noise and regularization, for Example 1.

(A) (B)

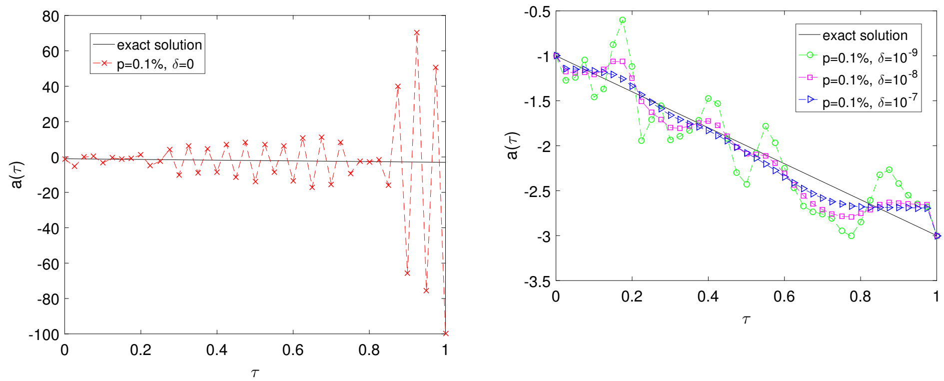

FIGURE 5. The exact (57) and approximate solutions of the potential term $a(\tau)$, for $p = 0.1\%$, with $\delta \in \{0, 10^{-9}, 10^{-8}, 10^{-7}\}$, for Example 1.

(A) (B)

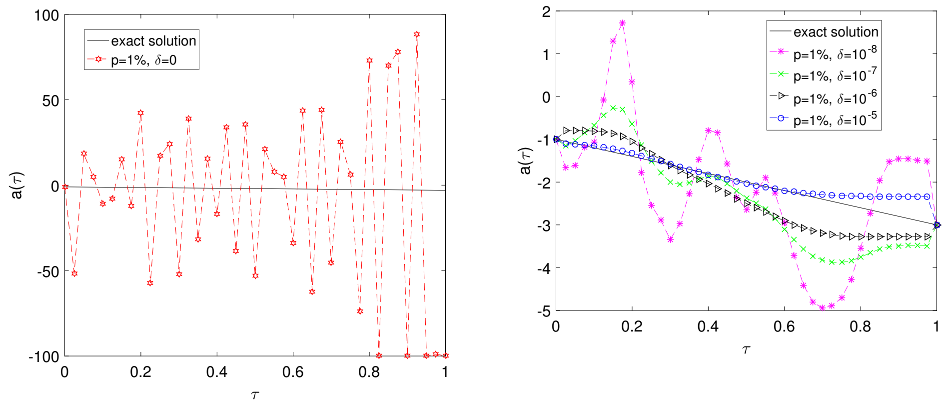

FIGURE 6. The exact (57) and approximate solutions of the potential term $a(\tau)$, for $p = 1\%$, with $\delta \in \{0, 10^{-8}, 10^{-7}, 10^{-6}, 10^{-5}\}$, for Example 1.

Next, we associate 0.1%, 1% noise with the measured data (4), as in equation (56). It is important to note that the inverse problem is not well posed therefore, we anticipate that the objective function (53) needs to be regularized for the sake of stability and accuracy in results. Figures 5 and 6 show visuals of the recovered source term $a(\tau)$. From Figures 5(a) and 6(a) it is clear that, as expected, for $\delta = 0$ we obtain inaccurate and unstable solutions with $\mathrm{RMSE}(a) = 27.7378$ for $p = 0.1\%$ and $\mathrm{RMSE}(a) = 52.8876$ for $p = 1\%$, respectively, as the problem is noise sensitive and ill-posed. Hence, regularization process is crucial for stable solutions. For this, the regularization parameter δ is chosen to be $10^{-9}, 10^{-8}, 10^{-7}$ for $p = 0.1\%$ noise (see Figure 5(b) obtaining RMSE$(a) \in \{0.3132, 0.1677, 0.1088\}$), and the regularization parameter $\delta \in \{10^{-8}, 10^{-7}, 10^{-6}, 10^{-5}\}$ for $p = 1\%$ noise (see Figure 6(b) obtaining RMSE$(a) \in \{1.3814, 0.7719, 0.4952, 0.2130\}$), which provide stable and comparitively accurate approximations for the function $a(\tau)$.

Other details about the no. of iterations, the minimum value of the cost function (53) at the last iteration, and the RMSE(a) (54) values, with and without regularization are listed in Table 6. Eventually, from Figures 4-6 and Table 6, it is observed that the MATLAB simulation results are fairly stable and accurate.

TABLE 6. RMSE values, no. of iterations and optimal value of the cost function (53) at last iteration, for $p \in \{0.1\%, 1\%\}$, with $\delta \in \{0, 10^{-9}, 10^{-8}, 10^{-7}, 10^{-6}, 10^{-5}, 10^{-4}\}$, for Example 1.

p	δ	RMSE(a)	Minimum value of (53)	Iter
0.1%	0	27.7378	4.3026E-12	100
	10^{-9}	0.3131	4.9701E-5	10
	10^{-8}	0.1677	5.8976E-5	10
	10^{-7}	0.1088	7.6486E-5	10
	10^{-6}	0.1600	1.8213E-4	10
1%	0	52.8876	5.8740E-4	400
	10^{-8}	1.3814	5.8000E-3	20
	10^{-7}	0.7719	6.3000E-3	20
	10^{-6}	0.4952	6.9000E-3	20
	10^{-5}	0.2130	8.7000E-3	20
	10^{-4}	0.3982	9.8200E-3	20

8.2. Example 2. In Example 1, smooth and linear coefficient given by equation (57) has been inverted. Now, we recover a nonlinear function for the potential term $a(\tau)$ in the problem (1)–(4) subject to following input data:

$$a(\tau) = 1 + \pi \cos^2(2\pi\tau), \quad \tau \in [0, 1]. \tag{60}$$

The analytical exact solution for $z(\kappa, \tau)$ is the same as that has been given in (51). The other input data is kept same as it was used in Example 1 and

$$f(\kappa, \tau) = \frac{\sin(\pi\kappa)\left(-\pi^2 - \tau^{1-\alpha}\right)}{\Gamma(2-\alpha) + (\tau - 1)(1 + \pi\cos^2(2\pi\tau))\sin(\pi\kappa)}, \quad \alpha \in (0, 1). \tag{61}$$

Tables 7 and 8 demonstrate the absolute errors between the analytical (51) and approximate solutions for $z(\kappa, \tau)$ with different values of α and $M = N \in \{60, 120\}$ at $\tau = 0.9$, for the forward problem (1)–(3), when $a(\tau)$ is known and given by (60). From these tables, we can see that the errors are reduced as the mesh sizes are decreased.

TABLE 7. The absolute errors between the approximate and analytical (51) solutions for $z(\kappa, \tau)$ with different values of $\alpha \in \{0.1, 0.4, 0.8\}$ and $M = N = 60$ at $\tau = 0.9$, for Example 2.

κ	Error $\alpha = 0.1$	Error $\alpha = 0.4$	Error $\alpha = 0.8$
0.1	3.2820E-4	3.5510E-4	3.6286E-4
0.2	6.2427E-4	6.7543E-4	6.9020E-4
0.3	8.5924E-4	9.2965E-4	9.4998E-4
0.4	1.0000E-3	1.1000E-3	1.1000E-3
0.5	1.1000E-3	1.1000E-3	1.2000E-3
0.6	1.0000E-3	1.1000E-3	1.1000E-3
0.7	8.5924E-4	9.2965E-4	9.4998E-4
0.8	6.2427E-4	6.7543E-4	6.9020E-4
0.9	3.2820E-4	3.5510E-4	3.6286E-4

TABLE 8. The absolute errors between the approximate and analytical (51) solutions for $z(\kappa, \tau)$ with different values of $\alpha \in \{0.1, 0.4, 0.8\}$ and $M = N = 120$ at $\tau = 0.9$, for Example 2.

κ	Error $\alpha = 0.1$	Error $\alpha = 0.4$	Error $\alpha = 0.8$
0.1	1.4743E-4	1.6118E-4	1.6550E-4
0.2	2.8043E-4	3.0658E-4	3.1481E-4
0.3	3.8598E-4	4.2197E-4	4.3330E-4
0.4	4.5375E-4	4.9606E-4	5.0937E-4
0.5	4.7710E-4	5.2159E-4	5.3558E-4
0.6	4.5375E-4	4.9606E-4	5.0937E-4
0.7	3.8598E-4	4.2197E-4	4.3330E-4
0.8	2.8043E-4	3.0658E-4	3.1481E-4
0.9	1.4743E-4	1.6118E-4	1.6550E-4

With the above data, the conditions of Theorem 4.1 can also be verified to affirm that we have unique solution to the problem. The initial approximation for $\underline{a}$ is supposed to be

$$a^0(\tau_n) = a(0) = 1 + \pi, \quad n = 1, 2, ..., N. \tag{62}$$

Next, we solve the problem (1)–(4) by setting $M = N = 40$, $\alpha = 0.5$ and $p = 0$ to reconstruction the unknown source term $a(\tau)$ along with the function $z(\kappa, \tau)$ for the exact input data. The corresponding approximate solutions for $a(\tau)$ is illustrated in Figure 7. It is observed that by (55) there is no numerical simulation of random noise with RMSE(a)=0.0734.

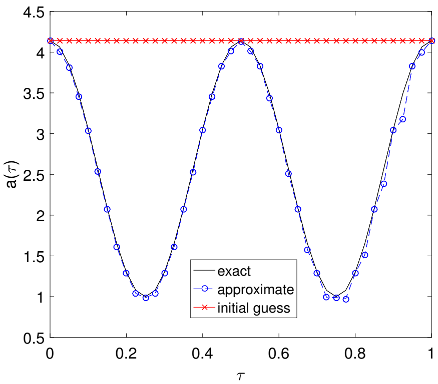

FIGURE 7. The approximate and analytical (60) exact curves for the potential term $a(\tau)$, for Example 2, in absence of noise.

Now, we discuss the case of noisy input data with $p \in \{0.01\%, 0.1\%\}$ by including Gaussian random noise in $r(\tau)$. As anticipated earlier, in absence of regularization, i.e., $\delta = 0$, the least-squares minimization returns an unstable solution. Hence, for restoration of the stability, we need to utilize the Tikhonov regularization approach by entering the stabilizer term in F (53). The exact (60) and approximate solutions for $a(\tau)$, before and after regularization are depicted in Figures 8 and 9. From Figures 8(a) and 9(a), it can be observed that the unstable (highly oscillatory) and inaccurate results are obtained for $a(\tau)$, if no regularization is installed with $\mathrm{RMSE}(a) = 3.1517$ for $p = 0.01\%$, and $\mathrm{RMSE}(a) = 28.4457$ for $p = 0.1\%$. In order to stabilise the coefficient $a(\tau)$, we employed regularization with $\delta \in \{10^{-11}, 10^{-10}, 10^{-9}\}$ (see From Figures 8(b)), obtaining $\mathrm{RMSE}(a) \in \{0.2571, 0.2135, 0.3293\}$ for $p = 0.01\%$, and $\delta \in \{10^{-10}, 10^{-9}, 10^{-8}\}$ (see From Figures 9(b)), obtaining $\mathrm{RMSE}(a) \in \{0.8767, 0.3710, 0.5784\}$ for $p = 0.1\%$. The exact (51) and numerically approximated solutions for $z(\kappa, \tau)$, before and after regularization, is plotted in Figure 10, where the contribution of $\delta > 0$ in curtailing the instability of the reconstructed temperature can be noted. For completeness, other RMSE values and the optimal value of cost function F at last iteration, before and after regularization are listed in Table 9. From table, it is obvious that the RMSE values for $a(\tau)$ are decreased as the minimum value of (53) increases. Overall, the computational outcomes produced by the CB-spline collocation approach together with Tikhonov's regularization advocate that stable and accurate numerical solutions can be achieved for the ill-posed third-order time-fractional pseudo-parabolic equation.

TABLE 9. The RMSE values, for $p \in \{0.01\%, 0.1\%\}$, before and after regularization, for Example 2.

$p = 0.01\%$	$\delta = 0$	$\delta = 10^{-11}$	$\delta = 10^{-10}$	$\delta = 10^{-9}$	$\delta = 10^{-8}$
RMSE(a)	3.1517	0.2571	0.2135	0.3293	0.4243
$p = 0.1\%$	$\delta = 0$	$\delta = 10^{-10}$	$\delta = 10^{-9}$	$\delta = 10^{-8}$	$\delta = 10^{-7}$
RMSE(a)	28.4457	0.8767	0.3710	0.5784	0.6128

(A) (B)

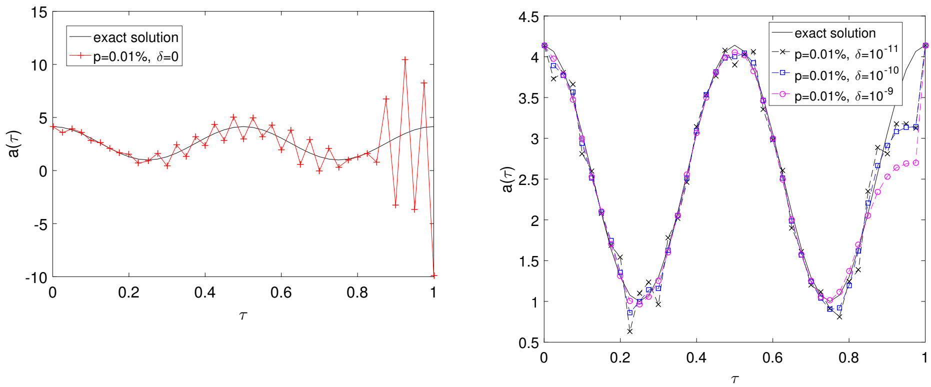

FIGURE 8. The approximate and analytical (60) exact curves for the potential term $a(\tau)$, for Example 2, with $p = 0.01\%$, before and after regularization.

(A) (B)

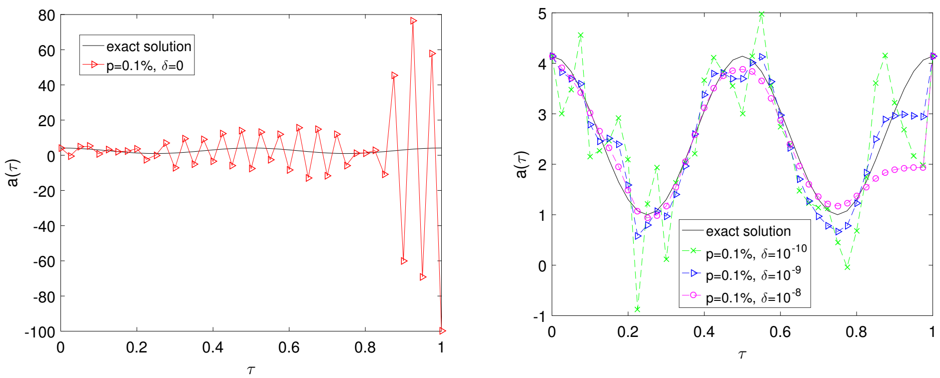

FIGURE 9. The approximate and analytical (60) exact curves for the potential term $a(\tau)$, for Example 2, with $p = 0.1\%$, before and after regularization.

9. Conclusions

The article considers the problem of identifying the timewise potential term for the third order time fractional pseudoparabolic equation with initial and homogeneous boundary conditions and the additional data at the left boundary of the space interval as an over-determination condition. The unique solvability theorem of the solution of the problem on a sufficiently small time interval is proved by using of the contraction principle. The stability results for the inverse fractional problem was

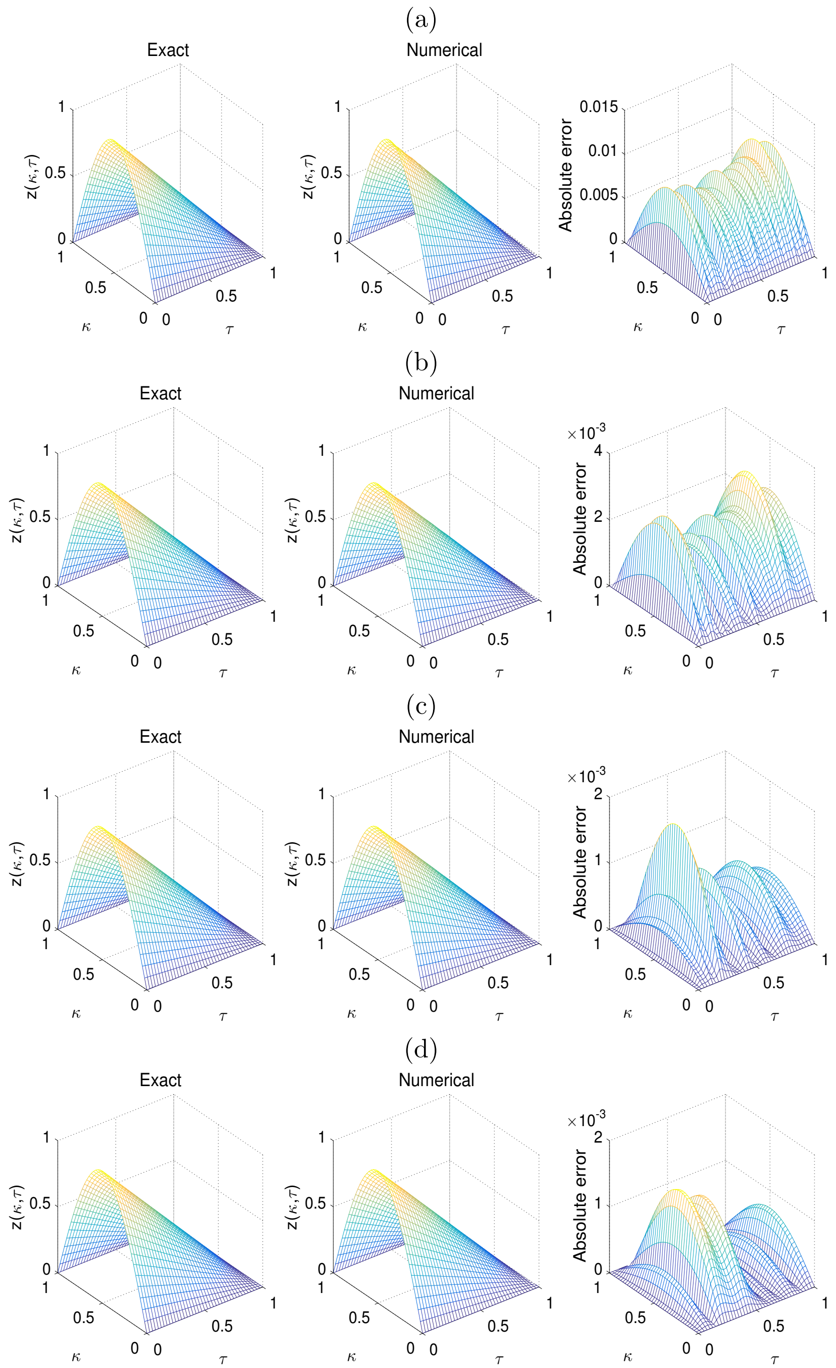

FIGURE 10. The numerical and exact (51) solutions for $z(\kappa, \tau)$, for Example 2 with $p = 0.1\%$, $\delta = 0, 10^{-10}, 10^{-9}, 10^{-8}$ and the absolute computational error between them.

presented. The presented work is novel and has never been solved numerically nor theoretically before. The direct solver based on the CB-spline collocation technique was employed. The stability analysis of the numerical solution has been investigated using the Fourier method. The resulting non-linear optimization problem was solved computationally by means of the MATLAB subroutine *lsqnonlin*. Since the problem under consideration was ill-posed, hence, the Tikhonov regularization was utilized in order to tackle the stability. The numerical results for the time fractional third order pseudoparabolic problem show that stable and accurate approximate results have been attained.

Funding statement. The authors received no specific funding for this study.

Declaration of interests. The authors declare that they have no known competing financial interests or personal relationships that could have appeared to influence the work reported in this paper.

References

[1] M. Amin, M. Abbas, D. Baleanu, M.K. Iqbal, M.B. Riaz, Redefined extended Cubic B-spline functions for numerical solution of time-fractional telegraph equation, *Computer Modeling in Engineering and Sciences* **127** (2021), 361–384.

[2] M. Amin, M. Abbas, M.K. Iqbal, D. Baleanu, Non-polynomial quintic spline for numerical solution of fourth-order time fractional partial differential equations, *Advances in Difference Equations* **2019** (2019), no. 1, 1–22.

[3] M. Amin, M. Abbas, M.K. Iqbal, D. Baleanu, Numerical treatment of time-fractional Klein-Gordon equation using redefined extended cubic B-spline functions, *Frontiers in Physics* **8** (2020), 288.

[4] A. Apelblat, Differentiation of the Mittag-Leffler functions with respect to parameters in the Laplace transform approach, *Mathematics* **8** (2020), no. 5, 657.

[5] A. Atangana, D. Baleanu, New fractional derivatives with nonlocal and non-singular kernel: Theory and application to heat transfer model, *Thermal Science* **20** (2016), 763–769.

[6] S. Aziz, A.M. Salman, Identification of an unknown source term for a time fractional fourth-order parabolic equation, *Electronic Journal of Differential Equations* **2016** (2016), 1–20.

[7] O. Bazighifan, Oscillatory applications of some fourth?order differential equations, *Mathematical Methods in the Applied Sciences* **43** (2020), no.17, 10276–10286.

[8] M.A. Hamed, A.A. Nepomnyashchy, Groove growth by surface subdiffusion, *Physica D: Nonlinear Phenomena* **298** (2015), 42–47.

[9] M.J. Huntul, N. Dhiman, M. Tamsir, Reconstructing an unknown potential term in the third-order pseudo-parabolic problem, *Computational and Applied Mathematics* **40** (2021), 140.

[10] M.J. Huntul, M. Tamsir, N. Dhiman, An inverse problem of identifying the time-dependent potential in a fourth-order pseudo-parabolic equation from additional condition, *Numerical Methods for Partial Differential Equations* **39** (2023), no. 2, 848–865.

[11] M.J. Huntul, Determination of a time-dependent potential in the higher-order pseudo-hyperbolic problem, *Inverse Problems in Science and Engineering* **29** (2021), no. 13, 3006–3023.

[12] K.A. Hussain, F. Ismail, N. Senu, Direct numerical method for solving a class of fourth-order partial differential equation, *Global J. Pure Applied Math* **12** (2016), 1257–1272.

[13] M.K. Iqbal, M. Abbas, I. Wasim, New cubic B-spline approximation for solving third order Emden-Flower type equations, *Applied Mathematics and Computation* **331** (2018), 319–333.

[14] M.I. Ismailov, Direct and inverse problems for thermal grooving by surface diffusion with time dependent Mullins coefficient, *Mathematical Modelling and Analysis* **26** (2021), 135–146.

[15] N. Khalid, M. Abbas, M.K. Iqbal, D. Baleanu, A numerical investigation of Caputo time fractional Allen-Cahn equation using redefined cubic B-spline functions, *Advances in Difference Equations* **2020** (2020), 1–22.

[16] A.A.Kilbas, H.M. Srivastava, J.J. Trujillo, *Theory and applications of fractional differential equations*, **204**, Elsevier Science, 2006.
[17] N.H. Luc, L.N. Huynh, D. Baleanu, N.H Can, Identifying the space source term problem for a generalization of the fractional diffusion equation with hyper-Bessel operator, *Advances in Difference Equations* **2020** (2020), 23.
[18] Mathworks (2019) Documentation Optimization Toolbox-Least Squares (Model Fitting) Algorithms, available at www.mathworks.com/help/toolbox/optim/ug /brnoybu.html.
[19] Y.T. Mehraliyev, G.K. Shafiyeva, On an inverse boundary-value problem for a pseudoparabolic third-order equation with integral condition of the first kind, *Journal of Mathematical Sciences* **204** (2015), 343–350.
[20] Y.T. Mehraliyev, G.K. Shafiyeva, Determination of an unknown coefficient in the third order pseudoparabolic equation with non-self-adjoint boundary conditions, *Journal of Applied Mathematics* **2014** (2014), 1–7.
[21] T.B. Ngoc, D. Baleanu, L.T.M. Duc, N.H. Tuan, Regularity results for fractional diffusion equations involving fractional derivative with Mittag-Leffler kernel, *Mathematical Methods in the Applied Sciences* **43** (2020), 7208–7226.
[22] I. Podlubny, *Fractional differential equations: an introduction to fractional derivatives, fractional differential equations, to methods of their solution and some of their applications*, Elsevier, 1998.
[23] M. Ruzhansky, D. Serikbaev, B.T. Torebek, N. Tokmagambetov, Direct and inverse problems for time-fractional pseudo-parabolic equations, *Quaestiones Mathematicae* **45** (2021), no. 7, 1–19.
[24] H. Tariq, G. Akram, Quintic spline technique for time fractional fourth?order partial differential equation, *Numerical Methods for Partial Differential Equations* **33** (2017), no. 2, 445–466.
[25] Y.L. You, M. Kaveh, Fourth-order partial differential equations for noise removal. *IEEE Transactions on Image Processing* **9** (2000), no. 10, 1723–1730.

(M.J. Huntul) Department of Mathematics, Faculty of Science, Jazan University, Jazan, Saudi Arabia
E-mail address: mhantool@jazanu.edu.sa

(I. Tekin) Department of Fundamental Sciences, Rafet Kayis Faculty of Engineering, Alanya Alaaddin Keykubat University, 07425 Antalya, Turkey
E-mail address: ibrahim.tekin@alanya.edu.tr

(M.K. Iqbal) Department of Mathematics, Government College University, Faisalabad, Pakistan
E-mail address: kashifiqbal@gcuf.edu.pk

(M. Abbas) Department of Mathematics, University of Sargodha, Sargodha, Pakistan
E-mail address: muhammad.abbas@uos.edu.pk